CAV2021
11th International Symposium on Cavitation
May 10-13, 2021, Daejeon, Korea

Computations of Cavitating Flows: Cryogenic Cavitation of Inducer and Supercavitating Underwater Vehicle

Hyunji Kim [1], Yohan Choe [1], Kyungjun Choi [1] and Chongam Kim [1,2]*

[1]Department of Aerospace Engineering, Seoul National University, Korea
[2]Institute of Advanced Aerospace Technology, Seoul National University, Korea

Abstract: This work presents computational results of cavitating flows in real engineering applications with complex geometries. The first application is cryogenic cavitating flows around turbopump inducer in liquid rocket engine. Using the real-fluid equation of state, thermal effect in cryogenic cavitation is successfully demonstrated with different types of working fluids and different inlet temperatures. Cavity formation and collapse around inducer is investigated with unsteady computations. The second application is supercavitating flows around a high-speed underwater vehicle with control fins. In order to validate the capabilities of the numerical solver for properly solving ventilated cavitating flows, computations are conducted and compared with experiments. Then, supercavitating flows around a high-speed underwater vehicle with control fins are computed to investigate the vehicle's hydrodynamic behaviors depending on freestream velocities, ventilation rates, and angles of attack. Both URANS and DES simulations are considered for the flow unsteadiness and detailed flow structures.

Keywords: Cryogenic cavitation; Supercavitation; Ventilated cavitation; Real-fluid EOS; Thermal effect

1. Introduction

In many engineering disciplines, cavitation is regarded as a detrimental phenomenon since it causes performance deterioration and structural damage in various hydraulic devices. In the same vein, cavitation around a turbopump inducer has been an obstacle in developing liquid rocket engines. A particular difficulty here is that cryogenic cavitating flows of liquid oxygen or hydrogen (commonly used liquid rocket propellants) yield very different characteristics from those in cold water due to the thermal effect. Unlike almost isothermal cavitation process in cold water, the temperature inside cryogenic cavity drops by a few degrees locally, which results in a significant change in the whole inducer performance. This work shows the capability that numerical analyses using general EOS could contribute to uncovering the cryogenic cavitation mechanism around the inducer, or at least, to predicting the cavity size under various operating conditions.

For high-speed underwater vehicles, however, cavitation can substantially reduce the drag force acting on the vehicle. Since a vehicle needs very high speed to achieve supercavitation with natural cavity, ventilated supercavitation is used at relatively low speed to achieve supercavitation safely. Since most of the previous numerical studies have focused on the maneuverability (and/or controllability) [1, 2] and natural supercaviating flows [3, 4] of the vehicles, it is essential to address ventilated supercavitating flow physics and the hydrodynamic characteristics of the vehicle with control fins. This work also presents extensive investigation of ventilated supercavitating flows around a high-speed underwater vehicle. RANS computations are performed to investigate the flow physics and hydrodynamic characteristics under various conditions such as freestream velocity, ventilation rate, and angle of attack. URANS and DES simulations are also conducted to understand flow unsteadiness and detailed flow structure inside/around the cavity.

* Corresponding Author: Chongam Kim, chongam@snu.ac.kr

2. Numerical Methods

One of the most popular numerical approaches for computing cavitating flows adopt volume- or mass-fraction equation with source terms accounting for the phase change rates. The present work adopts two mass-fraction equations to demonstrate concurrent natural and ventilated cavities around high-speed underwater vehicle. For accurate computations of cryogenic cavitating flows around inducer, a tabular form of real-fluid equation of state (EOS) is constructed based on NIST database. IAPWS97 formulations are employed as EOS for water. More descriptions on the flow solver can be found in [5].

3. Results

3.1. Cryogenic Cavitation around a Turbopump Inducer

A model inducer was experimented upon with cold water at the Korea Aerospace Research Institute (KARI), and the numerical predictions for the inducer performance agreed well with the experimental data [6]. Using the validated numerical solver, cryogenic cavitating flows have been computed for the same configuration. Table 1 summarizes the computational conditions.

Table 1. Flow conditions around inducer.

Case	Fluid	RPM	T_{in} (K)	Σ
A	Hydrogen	10,000	20.8	1.12×10^6
B	Oxygen	5,000	64.1	14.42
C			90	1.56×10^4
D	Water		305.4	14.22

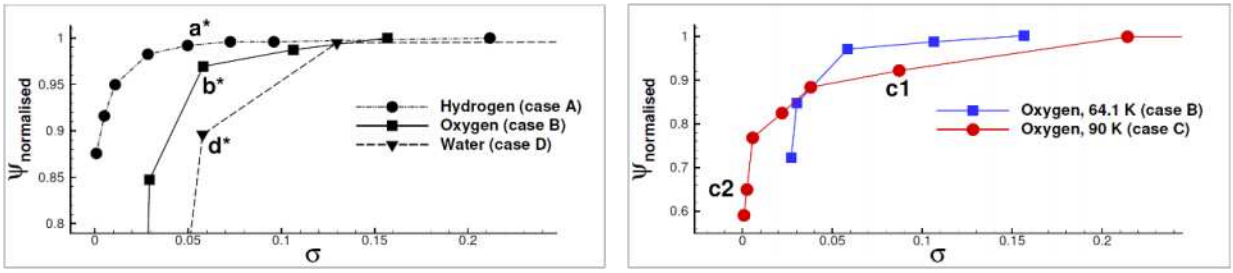

(**a**) (**b**)

Figure 1. Normalized head-rise coefficient of an inducer according to the tip cavitation number: (**a**) thermal effect according to working fluid (case: A, B, D); (**b**) effect of inlet temperature (case: B, C).

Figure 1 plots the head-rise coefficient Ψ in terms of the cavitation number σ. Here, Ψ is normalized by the value at the non-cavitating condition. As σ decreases by lowering the outlet pressure, cavitation occurs on the blade. The generation and collapse of the vapor volume disturbs the liquid flow and reduces the pumping capability of the inducer. Hydrogen flow characterized by high Σ (a crucial variable to determine thermal effect) shows a far delayed cavitation breakdown (i.e., total loss of pump capability). The gap between oxygen and water test cases under the same Σ conditions can be understood by the bubble growth theory [7]. Figure 1(b) presents the effect of inlet temperature on the same fluid (oxygen). The higher the temperature, the greater the thermal effect. To contrast the results before and after the breakdown, surface pressure distributions and the iso-surface of the vapor phase for points c1 and c2 are presented in Figure 2. Before the cavitation breakdown, cavities existed only locally near the leading-edge tip. After the

* Corresponding Author: Chongam Kim, chongam@snu.ac.kr

breakdown occurred, the cavities not only covered the blade surface but also almost blocked the whole passageway. **More analysis including unsteady computations will be given in the presentation.**

(**a**) (**b**)

Figure 2. Surface pressure and iso-surface of $\alpha_v = 0.2$ for case C: **(a)** c1 in Fig. 1(b), **(b)** c2 in Fig. 1(b).

3.2. Ventilated supercavitating flows around a high-speed underwater vehicle

We also carry out computations of supercavitating flows around an underwater vehicle. Based on the computational results, we investigate the flow physics and hydrodynamic characteristics of the vehicle including the control fins. The target vehicle geometry presented in Figure 3 is selected by referring a study by Kim et al. [4]. As shown in the figure, the vehicle has a disc-shaped cavitator and four control fins that have their own number. Figure 4 shows the cavity shapes depending on the freestream velocity and Figure 5 summarizes the drag and lift coefficients. As the freestream velocity increases, the cavity evolves from partial-cavitation state to supercavitation state, enclosing a greater part of the vehicle. Thus, the drag coefficient decreases with increased freestream velocity. Even though the angle of attack is zero, substantial lift force is generated by the vertical control fins and the body at the transition state, due to the cavity being lifted up by the buoyant force. In the case of vehicle body, this asymmetric cavity covers a greater part of the upper surface than the lower surface. That means, relatively high pressure acts on the lower surface since the surface is exposed to water, not air. Thus, the body also generates substantial lift force at the transition state. In the presentation, RANS simulation results under various ventilation rates and angles of attack are included. Also, both URANS and DES simulations are presented to show flow unsteadiness and detailed flow structures around/inside the cavity.

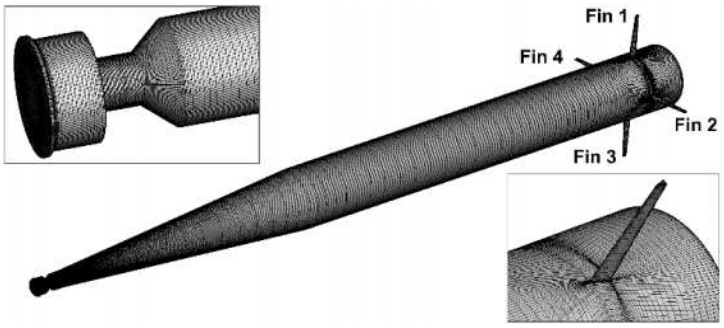

Figure 3. Target geometry

* Corresponding Author: Chongam Kim, chongam@snu.ac.kr

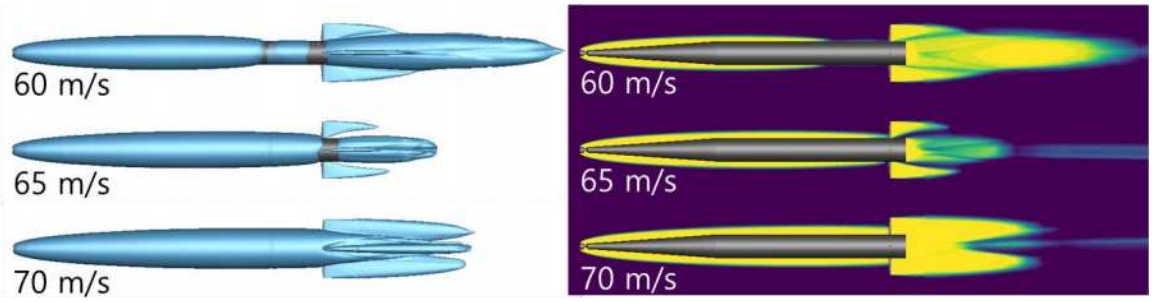

Figure 4. Cavity shapes depending on freestream velocity

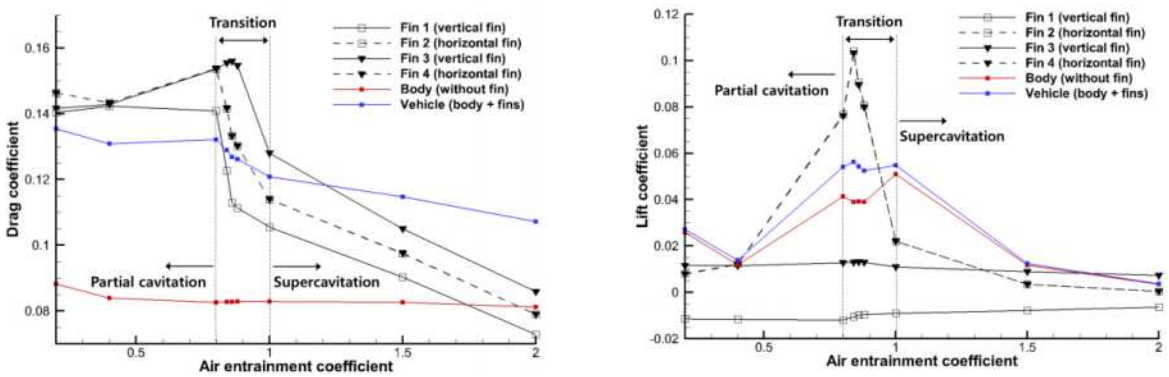

(a) Drag coefficient **(b)** Lift coefficient

Figure 5. Hydrodynamic coefficients

4. Conclusion

With a computational fluid dynamics tool, cavitating flows of industrial applications around 3-D complex geometries are successfully simulated and investigated.

Acknowledgments: The authors appreciate the support by Development of Next Generation Pipeline Robot Technology for the Long-Distance Inspection of the Low Pressure / the Low Flow of Gas Pipelines (RD2019-0251) from Korea Gas Corporation (KOGAS), by Korea Institute of Science and Technology Information (KSC-2020-CRE-0220), and by Institute of Advanced Aerospace Technology.

References

1. Yu, K.; Zhang, G.; Zhou, J.; Zou, W.; Li, Z. Numerical Study of the Pitching Motions of Supercavitating Vehilces. *Journal of Hydrodynamics, Ser. B* **2012**, *24*, 951-958.
2. Zou, W.; Yu, K.; Arndt, R.E.A. Modeling and Simulations of Supercavitating Vehicle with Planing Force in the Longitudinal Plane. *Applied Mathematical Modelling* **2015**, *39*, 6008-6020.
3. Yuan, X.; Xing, T. Hydrodynamic Characteristics of a Supercavitating Vehicle's aft body. *Ocean Engineering* **2016**, *114*, 37-46.
4. Kim, H.T.; Choi, E.J.; Kang, K.T.; Yoon, H.G. Numerical Anlaysis of the Cavitation Around an Underwater Body with Control Fins. *Journal of the Society of Naval Architects of Korea* **2019**, *56*, 298-307.
5. Kim, H.; Choe, Y.; Kim, H.; Min, D.; Kim, C. Methods for compressible multiphase flows and their applications. *Shock Waves* **2019**, *29*, 235-261.
6. Kim, H.; Kim, H.; Kim, C. Computations of Homogeneous Multiphase Real Fluid Flows at All Speeds. *AIAA Journal* **2018**, *56*, 2623-2634.
7. Brennen, C.E. *Cavitation and Bubble Dynamics.*; Cambridge University Press, 2014.

* Corresponding Author: Chongam Kim, chongam@snu.ac.kr